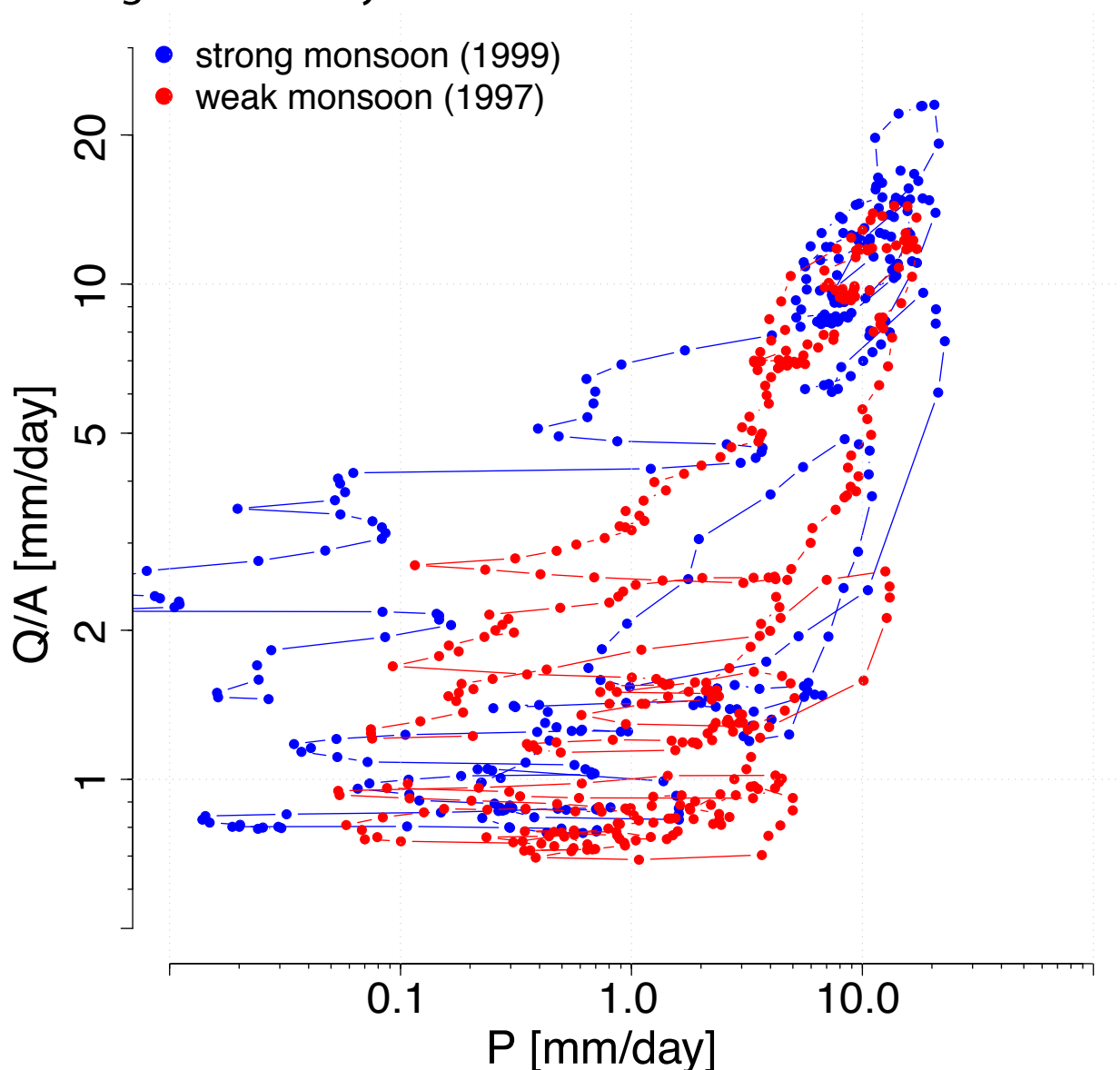
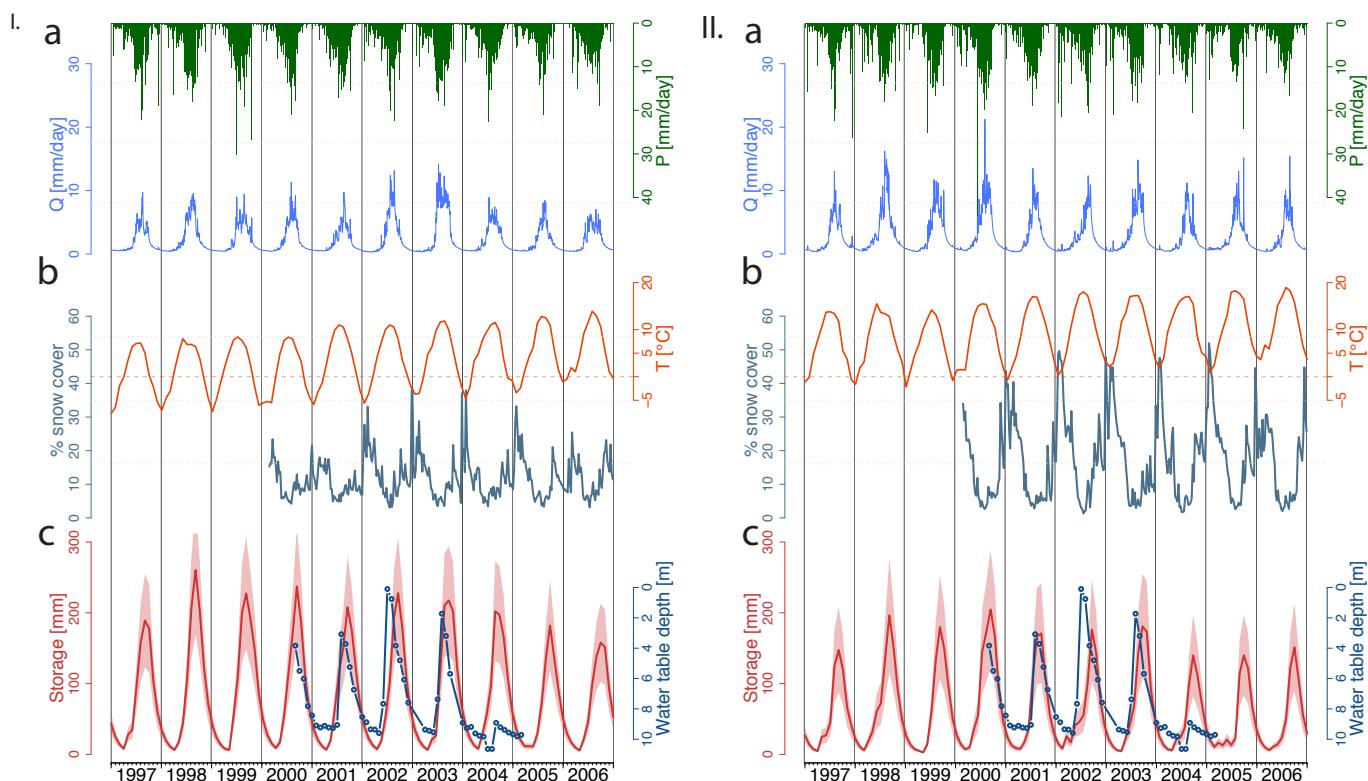


## Impact of transient groundwater storage on the discharge of Himalayan rivers



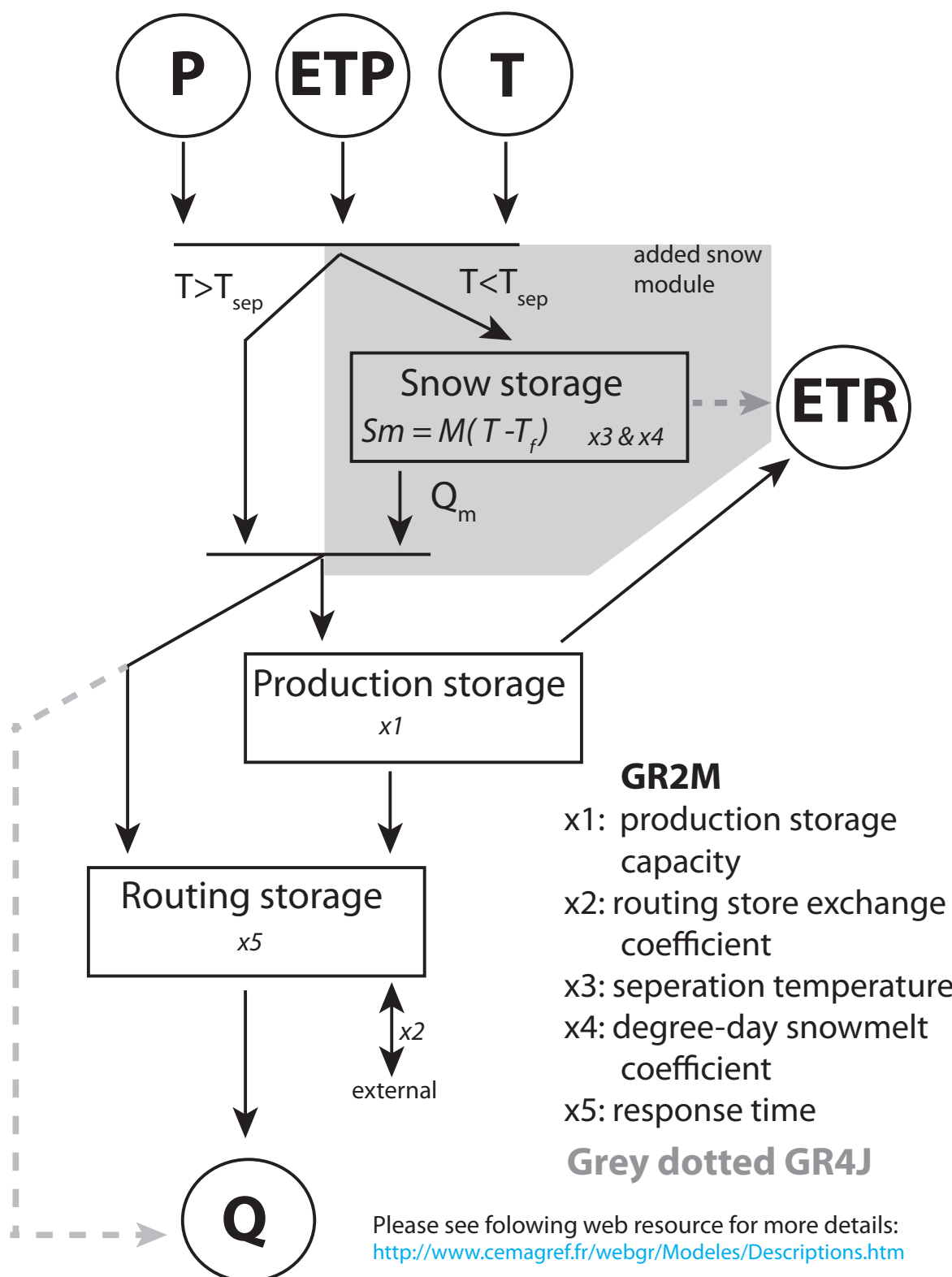
**S1| Difference between strong and weak monsoon hysteresis loops.** Precipitation-discharge hysteresis loop for the strong monsoon year 1999 and the weak monsoon year 1997<sup>11</sup> for the Narayani Basin. Data has been filtered with a 5-day moving average to avoid small-scale noise. The amplitude of the hysteresis loop is larger during strong monsoon years compared to weak ones.  $Q/A$  is the specific discharge,  $P$  is the mean basin precipitation.



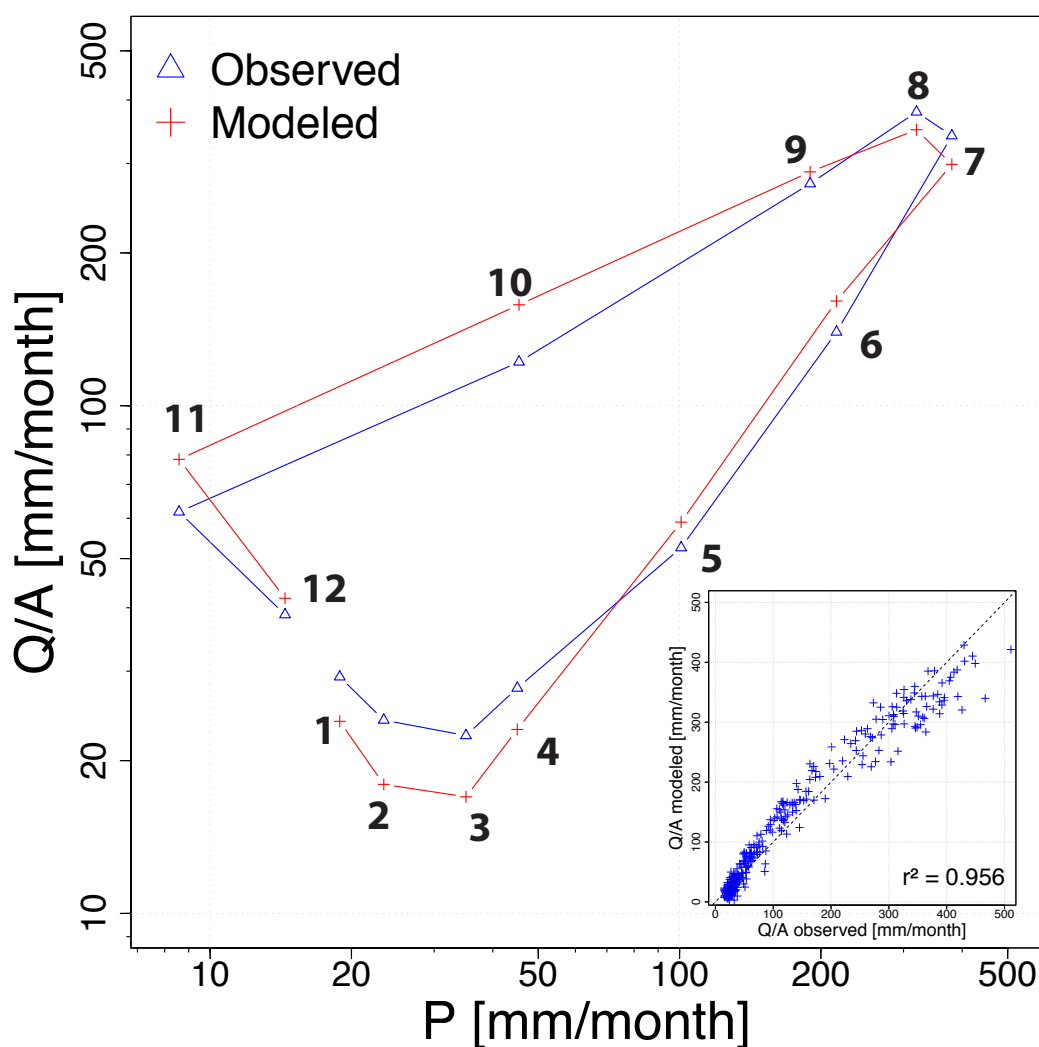
**S2| 10-year (1997-2006) temporal variability of several hydrological discharge cycle compartments, Koshi Basin (I) and Karnali Basin (II), central Nepal.** a, Daily precipitation (green), and daily specific river discharge (blue). b, Temperature (orange) as a glacier melt proxy (from CRU<sup>26</sup>) and percentage of basin-wide snow cover (dark green, data from MOD10C2 v.5<sup>27</sup> with an 8-day temporal resolution). c, Calculated groundwater storage evolution (red) derived from a modified version of the conceptual hydrological model GR2M<sup>18</sup> (see methods), shading illustrating model uncertainty, and ground water table variation (dark blue) observed in dug-wells in the Jhikhu Khola Basin<sup>22</sup> (station no. 1).

### Uncertainty estimation:

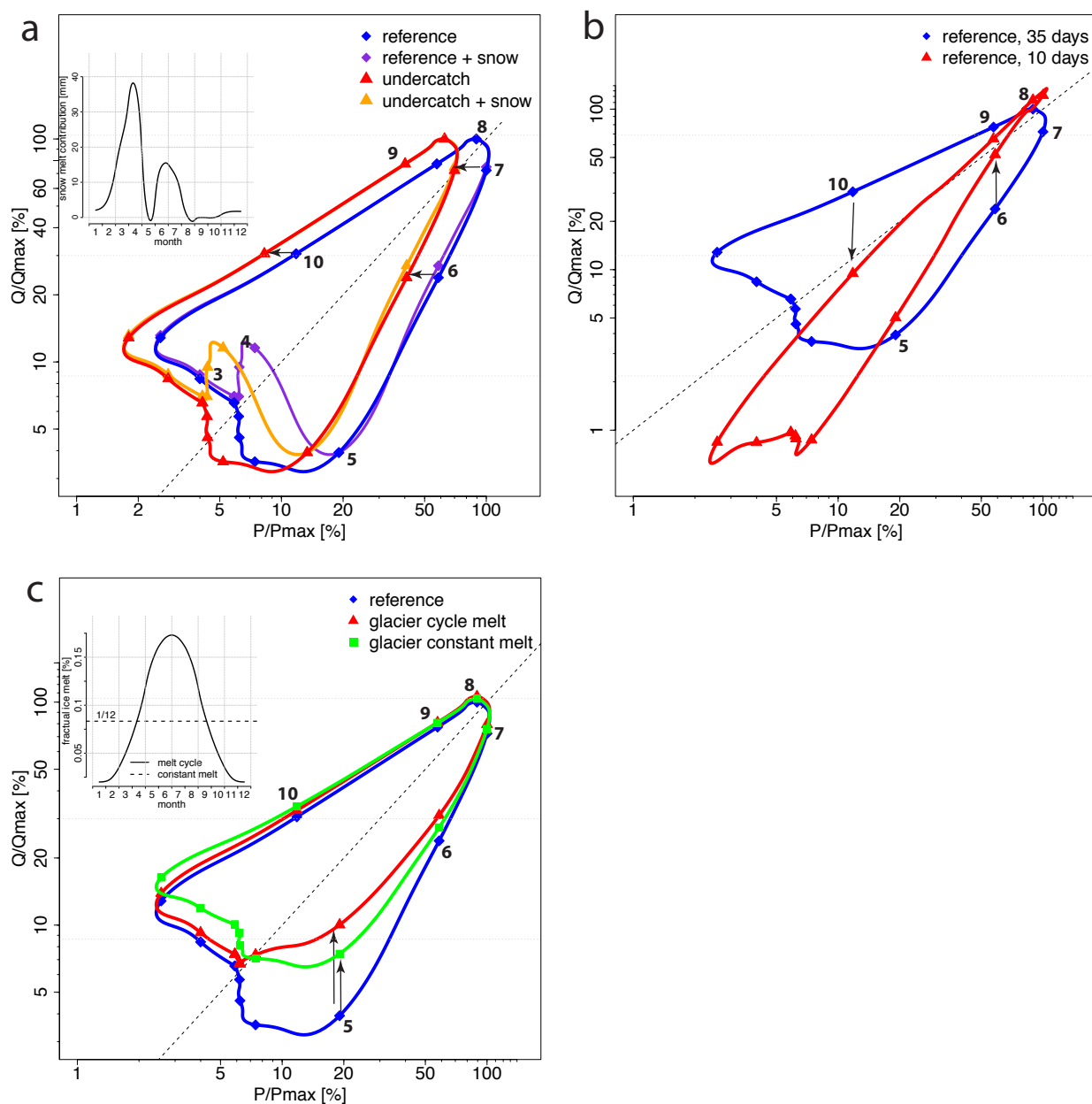
A Monte-Carlo approach is carried out to quantify the impact of observation data uncertainties on modeled groundwater properties (storage capacity, response time, see Table 1). Multiplicative errors have been considered for rainfall and discharge. Rainfall might be systematically underestimated by 30%<sup>10</sup>, and discharge biased by  $\pm 5\%$ . Conversely, ET and temperature errors are taken as additive, based on differences between independent datasets. Model is then recalibrated, model structure error is therefore not considered in this uncertainty analysis. While groundwater storage capacity is highly sensitive to systematic bias in precipitation data, recession curves, and therefore time response, are rather well constrained (Table 1).



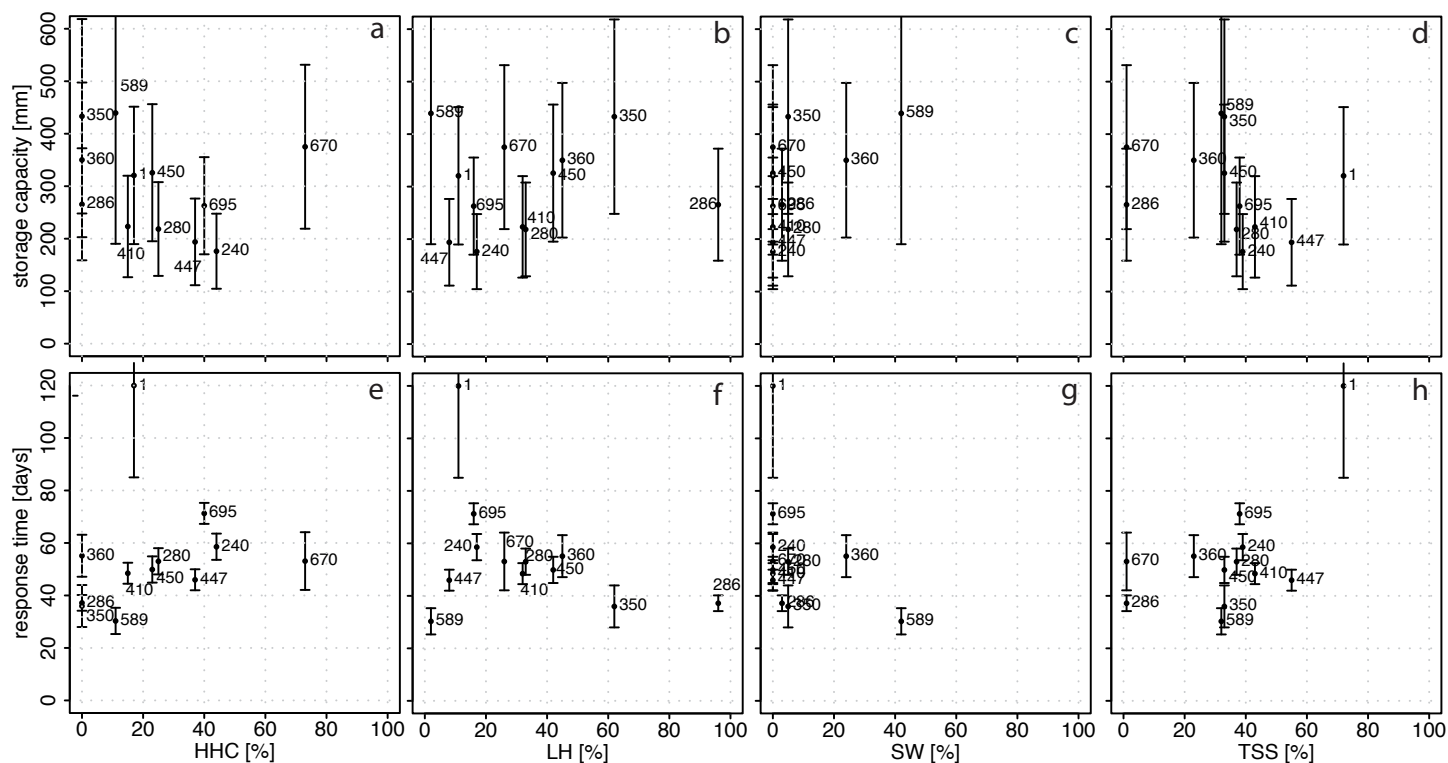
**S3| Flowchart of the modified version of the conceptual hydrological model used in this study.** Simplified schema of the conceptual models GR2M and GR4J<sup>18</sup>, and the added snow module. Black lines applied for both models GR2M and GR4J whereas gray dotted lines applied only for model GR4J. Please refer to Mouelhi et al. 2006 (ref. 18), the method section and the following web resource <http://www.cemagref.fr/webgr/Modelesgb/descriptionsgb.htm> for more detailed information.



**S4| Modeled vs. observed hysteresis loop for Narayani catchment (450).** Data are plotted on a monthly scale. The inset shows the linear correlation between the observed and modeled discharge. Q/A is the specific discharge. P is the monthly basin-wide precipitation rate.



**S 5| Influence of precipitation undercatch, snow melt, reservoir residence time and glacier melt on the shape of hysteresis loops.** The months are indicated by numbers. In all the examples, the mean monthly precipitation-discharge values for Rapti River at station 360 are used as a reference (blue). a, Effect of a constant 30% undercatch of precipitation and impact of snowmelt contribution, considering an annual water equivalent of the snowmelt contribution after the GLDAS-NOAH model25 (inset). b, Impact of the basin-wide storage capacity on the hysteresis shape of the Rapti catchment, considering characteristic basin response times of 35 days and of only 10 days, corresponding to a 20-fold downsizing of the storage capacity (see Methods). c, Influence of a 100 mm yr<sup>-1</sup> glacier melt contribution (or storage), considering a constant melt rate, equally distributed over the whole year or assuming a cyclic, temperature-driven ice melt contribution (both illustrated in the inset).



**S6 | Comparison between groundwater storage properties and geological units within the studied drainage basins.** Graphs illustrate storage properties (response time and storage capacity), plotted against geological units.

Station No.	240	280	286	350	360	410	447	450	670	695	589	1
Basin	Karnali	Karnali	Saradha	Rapti	Rapti	Kali Gandaki	Trishuli	Narayani	Dudh Koshi	Sapta Koshi	Bagmati	Jhikhu Khola
ETR [mm yr <sup>-1</sup> ]*	304	<b>407</b>	576	630	607	359	258	<b>457</b>	643	<b>591</b>	703	617
Nash-Sutcliffe coef.	0.73	<b>0.78</b>	0.8	0.84	0.84	0.84	0.48	<b>0.21</b>	0.75	<b>0.61</b>	0.61	0.12
Storage capacity [km <sup>3</sup> ]	4.0 ± 1.6	<b>8.9 ± 3.7</b>	0.2 ± 0.1	1.6 ± 0.7	1.8 ± 0.8	1.6 ± 0.7	0.8 ± 0.3	<b>9.9 ± 4</b>	1.0 ± 0.4	<b>9.9 ± 3.5</b>	1.4 ± 0.7	0.02 ± 0.01
Storage capacity [mm]	200 ± 75	200 ± 80	240 ± 90	425 ± 180	340 ± 140	220 ± 90	190 ± 80	310 ± 120	250 ± 100	170 ± 60	490 ± 90	210 ± 90
Estimated surface time response [days]	0.41	0.68	0.73	0.70	0.45	0.27	0.37	0.71	0.24	0.43	0.27	0.70
Estimated soil moisture time response [days]	7	7.6	3.8	8.3	5.8	7.8	6.9	7.4	5.1	10	9.5	12
t <sub>c</sub> GR4J [days]*	59 ± 13	47 ± 10	44 ± 6	63 ± 26	51 ± 22	54 ± 10	43 ± 6	36 ± 8	35 ± 25	66 ± 12	24 ± 5	120 ± 35
% snow-melt	12	<b>6</b>	n.a.	n.a.	n.a.	2	10	<b>2</b>	3	<b>2</b>	n.a.	n.a.
% discharge retarded	60	<b>65</b>	92	86	92	66	50	<b>68</b>	59	<b>60</b>	84	94

\* see Methods